https://doi.org/10.5194/egusphere-2026-1693
Preprint. Discussion started: 16 April 2026
© Author(s) 2026. CC BY 4.0 License.

Seven millennia of carbon accumulation in the Lower Danube Floodplain controlled by base-level change and anthropogenic forcing

Laurențiu Țuțuianu[1], Florin Zăinescu[2,1], Alfred Vespremeanu-Stroe[1,3], Ionel Stan[1], Mihaela Dobre[1,3], Maria Luca-Ilie[4], Gabriela Sava[4], Cristian Mănăilescu[4], Luminița Preoteasa[1,5]

[1]GEODAR Research Center for Geomorphology, Geoarchaeology, and Paleo-Environments, ICUB Research Institute of the University of Bucharest, Bucharest, Romania;

[2]Aix-Marseille University, CNRS, IRD, INRAE, Collège de France, CEREGE, Aix-en-Provence, France;

[3]Faculty of Geography, University of Bucharest, Bucharest, Romania;

[4]RoAMS Laboratory, Horia Hulubei National Institute for R&D in Physics and Nuclear Engineering, Măgurele, Romania;

[5]Sfântu Gheorghe Marine and Fluvial Research Station, University of Bucharest, Sf. Gheorghe, Romania

Correspondence to: Laurențiu Țuțuianu (laurentiu.tutuianu@drd.unibuc.ro)

Abstract

Floodplains are among the most important long-term terrestrial carbon sinks, yet the controls governing millennial-scale carbon accumulation remain poorly constrained, particularly in large fluvial systems. Here we reconstruct the history of organic carbon accumulation in the Lower Danube Floodplain (LDF), one of the largest floodplain systems in Europe, using stratigraphic and chronological data from eight sediment cores spanning the last 7000 years. Total organic carbon (TOC), grain-size distribution, dry bulk density, and sedimentation rates derived from Bayesian age–depth models were integrated to quantify temporal changes in carbon accumulation rates (CAR) and to evaluate the geomorphic and environmental controls governing long-term carbon burial.

Over the investigated period, large volumes of sediment accumulated across the LDF, forming a thick stratigraphic sequence that stores substantial amounts of organic carbon. However, long-term carbon burial did not occur at a constant rate but instead reflects three distinct phases controlled by changing boundary conditions. During the early part of the record, rapid floodplain aggradation associated with post-glacial base-level rise promoted efficient carbon burial through accelerated mineral sediment deposition despite relatively low organic carbon concentrations. Following base-level stabilization, sedimentation rates declined and the system shifted toward preservation-dominated sequestration, characterized by higher organic carbon contents but lower carbon accumulation efficiency under more stable hydrogeomorphic conditions. During the last two millennia, increasing human activity in the Danube basin enhanced sediment delivery, leading to a renewed increase in carbon burial despite declining organic carbon concentrations.

Superimposed on these millennial-scale trends, carbon burial also varies substantially among sedimentary facies, reflecting contrasting depositional environments and carbon sequestration mechanisms within the floodplain. Facies-based analyses reveal contrasting mechanisms of carbon storage across floodplain environments. Peat and organic-rich deposits exhibit the highest TOC values (average 17 %) but relatively moderate CAR due to low sediment accumulation rates, whereas paleochannel and overbank deposits achieve higher CAR through rapid burial of mineral sediments containing lower organic carbon concentrations. These results demonstrate that long-term floodplain carbon sequestration is governed by

https://doi.org/10.5194/egusphere-2026-1693
Preprint. Discussion started: 16 April 2026
© Author(s) 2026. CC BY 4.0 License.

the interaction between accommodation space, sedimentation rate, and hydrological connectivity rather than organic carbon concentration alone.

These findings highlight the importance of maintaining hydrological connectivity and sediment delivery in order to sustain carbon burial in large floodplain systems, suggesting that restoration strategies focused on reconnecting floodplain surfaces to fluvial processes may enhance long-term carbon sequestration and associated ecosystem services.

1 Introduction

River floodplains are among the most effective terrestrial environments for long-term carbon storage, playing a vital role in regulating the global carbon cycle. Although they occupy only 0.5–1% of the Earth's land surface, they store approximately 0.5–8% of the global soil organic carbon (Sutfin et al., 2016). This disproportionate contribution is driven by high productivity, periodic sediment deposition, and anoxic sediment conditions that limit organic matter decomposition, while the sediment deposition also buries plant litter and soil carbon, protecting it from oxidation and storing it for centuries to millennia.

Understanding carbon dynamics in floodplains has become increasingly relevant in the context of climate change. Since 1850, atmospheric CO_2 concentrations have increased by around 43%, from 287 ppm to over 410 ppm (Goosse et al., 2022; Ramonet et al., 2023), mainly due to fossil fuel combustion and land-use change (Ciais et al., 2013). This rise has driven global warming during the industrial period, with recent decades characterized by unprecedented temperature anomalies across large parts of the Northern Hemisphere (IPCC, 2021). In a longer-term perspective, this warming culminated in summer 2023 temperatures in the extra-tropical Northern Hemisphere exceeding 2 °C above the reconstructed average of the past 2,000 years (Esper et al., 2024). Identifying and conserving effective natural carbon sinks is therefore a priority in climate mitigation strategies (Fawzy et al., 2020).

Fluvial systems play a dual role in the terrestrial carbon cycle: they transport sediment and organic carbon from upland sources toward the ocean, while a substantial fraction is temporarily or permanently stored within floodplains and deltas (Hoffmann et al., 2013). At the global scale, river systems process and store significant amounts of organic carbon estimated at 0.5 to 1.6 Pg C yr^{-1} (Regnier et al., 2013). Their capacity to function as effective carbon sinks depends on hydrological connectivity and sediment supply. In unconfined floodplain systems, frequent overbank flows deliver fine-grained sediments and organic matter, promoting vertical accretion and long-term burial under low-oxygen conditions (Palomo & Niell, 2009; Rogers et al., 2019). However, river regulation, embankment, and land reclamation have substantially reduced these processes in many large river systems, diminishing their sediment and carbon storage capacity.

The Lower Danube Floodplain (LDF), located upstream of the Danube Delta apex, is one of Europe's most extensive semi-natural floodplain systems. Shaped by millennia of hydrological, climatic, and human influences, the LDF constitutes an important archive of environmental change. Carbon storage within the Danube catchment has been investigated in selected sites, either through Holocene-scale reconstructions of the sedimentary sequence at the river's headwaters (Hoffmann et al., 2009) or by quantifying organic carbon stocks within the uppermost meter of

https://doi.org/10.5194/egusphere-2026-1693
Preprint. Discussion started: 16 April 2026
© Author(s) 2026. CC BY 4.0 License.

floodplain soils, such as in the Donau-Auen National Park (Cierjacks et al., 2010). For the downstream floodplain, however, comparable studies are lacking. Aside from a few graphical datasets presented in Nowacki et al., (2019), Ţuţuianu et al., (2021), and Hanganu et al., (2023), little is known about carbon stocks or accumulation history in this region. This scarcity of integrated, stratigraphically constrained data limits our understanding of carbon sequestration dynamics and their environmental controls in one of Europe's largest remaining semi-natural floodplain systems.

Most studies that reconstruct Holocene-scale carbon storage have focused on lacustrine environments, peatlands, or coastal wetlands (Dong et al., 2021; Fujimoto et al., 2009; Longman et al., 2021; Panait et al., 2017). In contrast, fluvial floodplains remain underrepresented in regional and global carbon budgets, despite growing recognition of their importance (Sutfin et al., 2016; Wohl & Pfeiffer, 2018).

In this study, we aim to reconstruct total organic carbon (TOC) concentration and carbon accumulation rate (CAR) in the LDF over the past 7,000 years, and to explore their links to Black Sea level evolution and human activity in the Danube catchment. To this end, we integrate stratigraphic analyses from eight floodplain cores with 64 calibrated radiocarbon dates and derive a series of 1-kyr isochrones to quantify long-term carbon and sediment storage.

2 Study area

The study area extends over an approximately 100 km long sector of the LDF in southeastern Romania, stretching between Turcoaia and Tulcea (Fig. 1) and covering ~900 km². A significant portion of the floodplain is designated as a nature reserve and forms part of the Natura 2000 network (ROSPA0121 and ROSPA0031). The area can be broadly divided into two sections: (1) a natural floodplain sector (~120 km^2), located between the Danube Delta apex and the Isaccea promontory, characterized by numerous lakes (e.g., Rotundu, Telincea, Parcheş, Somova, and Babele), swamps, and fluvial channels; and (2) an artificially modified section, located between the Isaccea promontory and Turcoaia village, which was extensively drained and embanked during the 20th century for agricultural use, covering approximately 780 km².

At Tulcea, the Danube River exhibits a mean annual water discharge of ~6500 $m^3\ s^{-1}$ and a solid sediment load of ~600 $kg\ s^{-1}$, markedly lower than the ~1800 $kg\ s^{-1}$ recorded under semi-natural conditions prior to the construction of the Iron Gate I and II hydropower dams. These values are recorded downstream of the confluence with the final two major tributaries, the Siret River (254 $m^3\ s^{-1}$) and the Prut River (90 $m^3\ s^{-1}$) (Radoane, 2021; Romanescu, 2015).

The floodplain stratigraphy consists of well-defined sedimentary units. At depths greater than 30 meters, coarse sands and gravels – likely deposited during the Late Glacial – form the basal unit. These are overlain by finer sands and silts accumulated during the Early and Middle Holocene (cores 1-3, Fig. 1). The uppermost 5 to 8 meters, deposited over the past 5000 years, are composed predominantly of silt, with sand contributing slightly more than 10% of the total sediment composition (Fig. 1) (Ţuţuianu et al., 2021).

https://doi.org/10.5194/egusphere-2026-1693
Preprint. Discussion started: 16 April 2026
© Author(s) 2026. CC BY 4.0 License.

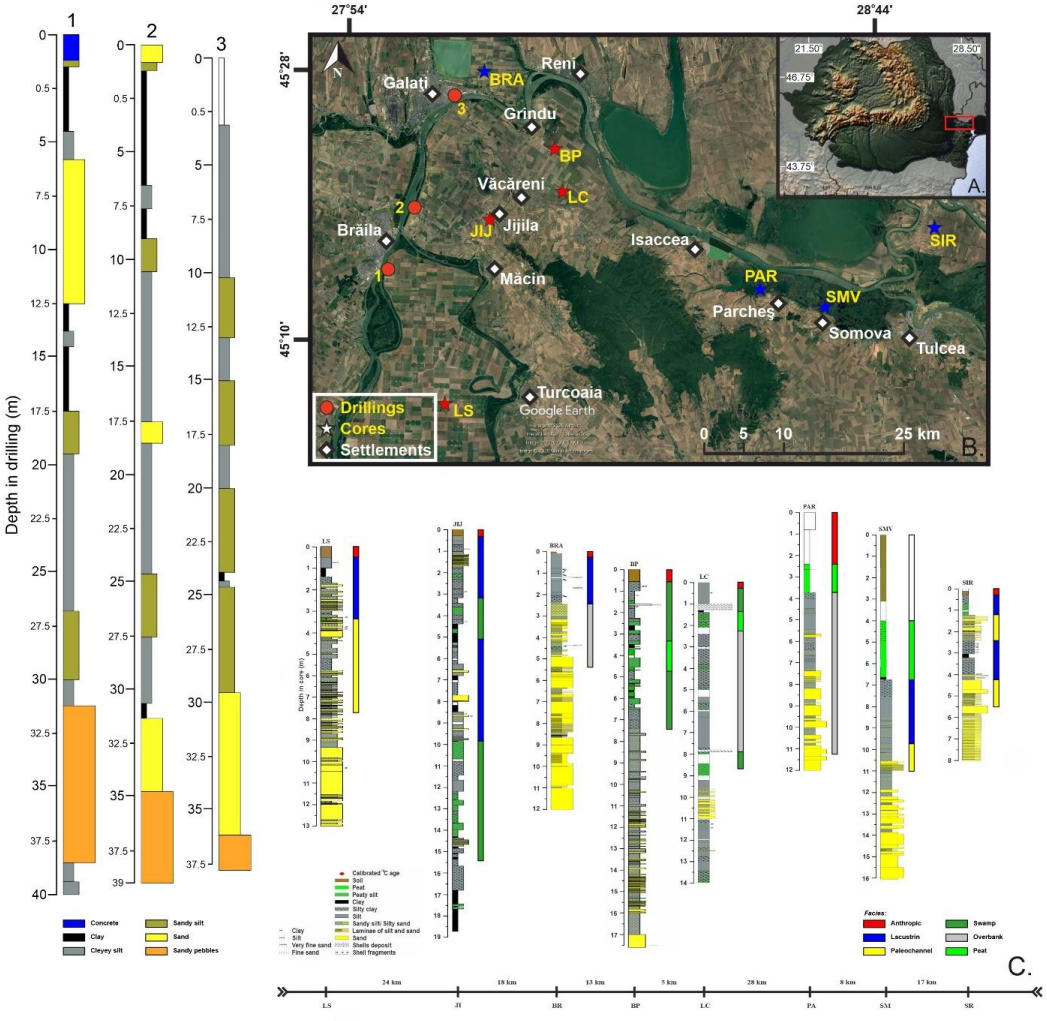

Figure 1. Distribution of sediment cores and stratigraphic framework of the LDF. (A) Location of the study area in SE Romania. (B) Spatial distribution of sediment cores shown on Google Earth satellite imagery (Maps data: ©Google Earth 2026; imagery: © Airbus, CNES/Airbus, Maxar Technologies, Landsat/ Copernicus): newly recovered (red stars) and previously published (blue stars). Historical ISPIF drillings are shown as red circles and nearby settlements as white diamonds. Core sites are labelled using abbreviations corresponding to site names: LS – Șerban Lake, JIJ – Jijila Lake, BRA – Brateș Lake, BP – Popina Swamp, LC – Crapina Lake, PAR – Parcheș, SMV – Somova, and SIR – Sireasa. (C) Floodplain stratigraphy along the river transect. Stratigraphic logs of the studied cores are shown below the map, with vertical colour bars indicating interpreted sedimentary facies.

In the second half of the 20th century, the LDF experienced extensive anthropogenic transformation (Constantinescu et al., 2015). Previously characterized by a mosaic of wetlands, interconnected lakes, swamps, and seasonal channels, the landscape was fundamentally altered

https://doi.org/10.5194/egusphere-2026-1693
Preprint. Discussion started: 16 April 2026
© Author(s) 2026. CC BY 4.0 License.

through the construction of embankments, drainage networks, and irrigation systems. These interventions converted large portions of the floodplain into arable land and disrupted natural sedimentation and hydrological processes across most of the area.

The local climate is classified as temperate dry, with mean annual temperatures ranging between 10–11°C. Annual precipitation averages between 450 and 500 mm, while potential evapotranspiration exceeds 700 mm (Sandu et al., 2008). As a result, the region experiences a persistent annual water deficit of 200–300 mm, which influences floodplain hydrology and vegetation (Busuioc et al., 2010).

3 Methodology

3.1 Site Selection

Eight sediment cores (Fig. 2) were selected to capture TOC and CAR variability across the LDF. Five cores were taken from artificially modified floodplain sectors converted to agriculture during the communist era, two from preserved natural floodplain zones, and one from a paleochannel estimated to be older than 6000 years.

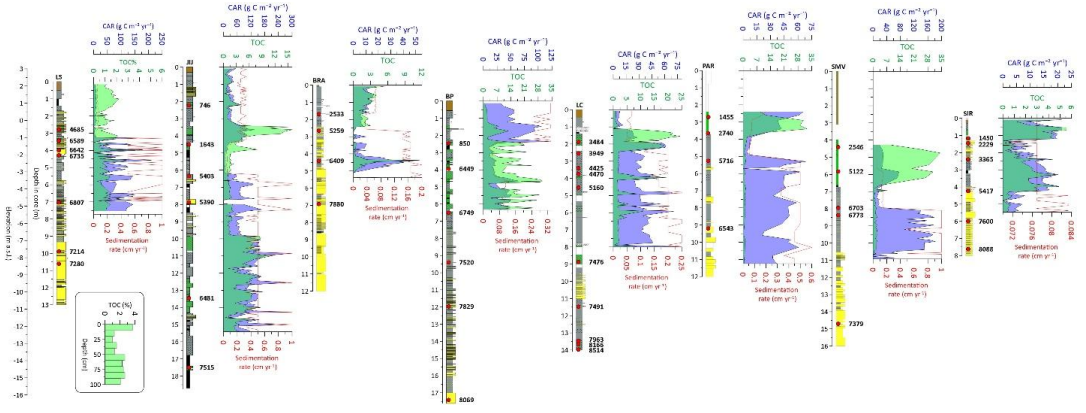

Figure 2. Stratigraphic logs and down-core variations in total organic carbon (TOC, %), carbon accumulation rate (CAR, g C m^{-2} yr^{-1}), and sedimentation rate (cm yr^{-1}) for the eight studied cores. Lithological columns are shown alongside TOC (green shading), CAR (blue shading), and modeled sedimentation rates (red dashed line) derived from Bayesian age–depth models. Radiocarbon ages (cal BP) are indicated along the stratigraphic profiles. Elevation is expressed relative to mean sea level. Inset: detailed variation of mean TOC values in 10-cm intervals within the upper 1 m of sediment cores from agricultural sectors of the floodplain, illustrating the decline in TOC concentrations within the upper 50 cm.

3.2 Core Collection

Cores were collected between 2016 and 2022 using a percussion corer system (Eijkelkamp Cobra TT), which operates with an internal hammer mechanism and is suitable for retrieving relatively undisturbed sediment cores from unconsolidated floodplain deposits. The cores were extracted in 1 m PVC liners with a diameter of 5 cm. After extraction, the PVC tubes were

https://doi.org/10.5194/egusphere-2026-1693
Preprint. Discussion started: 16 April 2026
© Author(s) 2026. CC BY 4.0 License.

transported horizontally to the laboratory, where they were split longitudinally. One half of each core was preserved in a core repository at a constant temperature of 4 °C for archival purposes, while the other half was visually described and subsampled for grain size analysis, loss-on-ignition (LOI), total organic carbon (TOC), and micropaleontological analyses (pollen, ostracods, and foraminifers), part of which has already been described in detail in Hanganu et al., (2023) and Țuțuianu et al., (2018).

3.3 Laboratory Analyses

Grain size analysis (n = 565) was performed with a Horiba LA950 laser diffractometer. Prior to measurement, samples were pretreated with 30% acetic acid and 10% hydrogen peroxide to remove carbonates and organic matter, followed by 2% sodium hexametaphosphate to prevent clay particle flocculation. Grain size parameters were calculated using the formulas of Folk & Ward, (1957) and processed in Gradistat v.8 software (Blott & Pye, 2001).

For LOI, 553 samples (~3 g each) were dried at room temperature for 48-72 hours and then subjected to a three-step thermal analysis. Samples were first heated at 105 °C for 24 hours to determine water content, then at 550 °C for 6 hours to estimate organic matter content (LOI_{550}), and finally at 950 °C for 2 hours to quantify inorganic carbonate content (Wang et al., 2011); all calculations were performed using the formulas of Heiri et al., (2001).

Bulk density was measured on 106 undisturbed samples, selected based on textural and organic matter variability. The samples were taken from the archived half of the cores stored at 4 °C, and represent 1 cm slices, dried at 105 °C for 24 hours before weighing. For the remaining intervals, bulk density was estimated using a regression-based equation adapted from Keogh et al., (2021), yielding a coefficient of determination of $R^2 = 0.77$:

$$\rho = a / (1 + a \times b \times LOI_{550}) + 0.07, \text{ where } a = 2.296 \text{ and } b = 0.139.$$

This combined approach allows for the construction of a complete, high-resolution bulk density profile, enabling accurate calculation of sediment and carbon accumulation rates, while remaining more efficient than direct measurement of the full dataset.

TOC content was directly measured in 221 duplicate samples using a Primacs MCS analyzer. In the first step, total carbon (TC) was determined by combusting the sample at 1000 °C. In the second step, a subsample was acidified with 20 % phosphoric acid to remove organic matter, then combusted to measure total inorganic carbon (TIC). TOC was calculated by subtracting TIC from TC (TOC = TC − TIC).

Based on TOC content and dry bulk density, together with sedimentation rates derived from Bayesian age–depth models (see below), carbon accumulation rates (CAR; g C m^{-2} yr^{-1}) were calculated as CAR = SR × ρ × TOC.

3.4 Organic Matter and TOC Correlation

To extrapolate TOC values from organic matter measurements across the full dataset, we developed a site-specific correlation equation based on paired LOI_{550} and TOC measurements of 221 samples. Two-thirds of the dataset were used to construct the regression model, while the

https://doi.org/10.5194/egusphere-2026-1693
Preprint. Discussion started: 16 April 2026
© Author(s) 2026. CC BY 4.0 License.

remaining third served for validation. The resulting regression equation (TOC = -0.7476 + 0.4702 × LOI_{550}) shows a strong linear correlation (R^2 = 0.90), supporting the use of this equation to extrapolate TOC values from LOI data across the full dataset (Fig. 3).

This approach was preferred over the commonly used van Bemmelen conversion factor (1.724), which assumes a fixed carbon content of 58% in organic matter. However, this assumption has been widely criticized for its limited applicability across sediment types and depositional environments. As shown by Pribyl (2010), the effective conversion factor may vary substantially – from below 1.4 to above 2.5 – depending on the composition, oxidation state, and origin of the organic matter. This variability underscores the importance of site-specific calibrations in sedimentary systems.

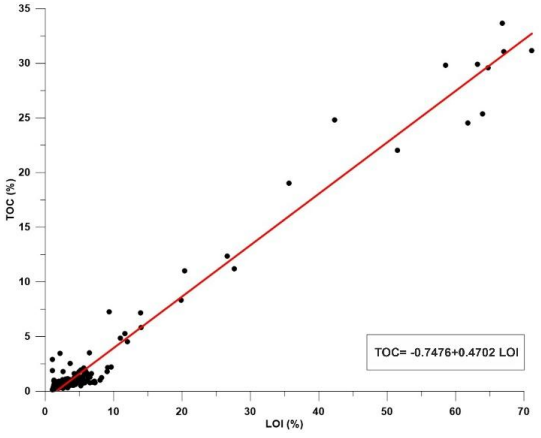

Figure 3. Simple linear regressions of TOC against LOI

The validated regression equation was subsequently applied to all LOI_{550} measurements to estimate TOC concentrations along the core profiles (Fig. 3).

3.5 Isochrone Configuration

Radiocarbon dating (Table 1) was used to establish a chronological framework for sediment deposition. Measurements were performed in two distinct laboratories, namely, RoAMS Laboratory of „Horia Hulubei" National Institute for R&D in Physics and Nuclear Engineering (IFIN-HH), Romania, and the Radiocarbon and Mass Spectrometry Laboratory, Silesian University of Technology, Gliwice, Poland.

Sample ID	Laboratory code	Depth (cm)	^{14}C age (years BP)	±	Comments
LS 1	5620.1	112	3560	89	outlier
LS 2	5622.1	278	4147	51	
LS 3	LS_343	343	5789	38	
LS 4	958.66	400	5831	41	
LS 5	5025.1	428	5916	36	
LS 6	957.66	703	5973	38	
LS 7	LS_863	863	5943	37	outlier
LS 8	5026.1	988	6305	32	
LS 9	5027.1	1060	6357	30	
Jij 1	Jij_222	222	849	21	
Jij 2	Jij_380	380	2206	24	outlier
Jij 3	5029.1	450	1755	32	
Jij 4	Jij_480	480	902	28	outlier
Jij 5	1085.66	634	4644	37	
Jij 6	Jij_786	786	4683	26	
Jij 7	1086.66	872	3715	36	outlier

https://doi.org/10.5194/egusphere-2026-1693
Preprint. Discussion started: 16 April 2026
© Author(s) 2026. CC BY 4.0 License.

Jij 8	5623.1	1263	3635	45	outlier
Jij 9	Jij_1345	1345	5703	30	
Jij10	Jij_1625	1625	7488	31	outlier
Jij 11	1089.66	1749	6635	41	
Bra_62*	946.66	168	2452	37	
Bra_60*	GdA-5544	265	4590	35	
Bra_65*	GdA-5545	440	5650	30	
Bra_68*	GdA-5545	692	7060	40	
Bra_69*	947.66	782	6660	158	outlier
BP 1	1274.66	246	952	28	
BP 2	5691.1	292	4352	40	outlier
BP 3	5692.1	393	5670	41	
BP 4	BP_441	441	4587	31	outlier
BP 5	951.66	650	5925	51	
BP 6	BP_939	939	6643	46	
BP 7	950.66	1195	6999	56	
BP 8	948.66	1740	7243	63	
LC 1	5337.1	188	3272	31	
LC 2	LC_254	254	3635	37	
LC 3	5328.1	340	3960	34	
LC 4	5329.1	374	3980	27	
LC 5	955.66	397	4835	47	outlier
LC 6	5338.1	453	4476	34	
LC 7	1275.66	630	2046	32	outlier
LC 8	954.66	886	6573	71	
LC 9	953.66	1147	6597	48	
LC 10	LC_1345	1345	7142	51	
LC 11	5333.1	1366	7364	38	
LC 12	952.66	1397	7744	52	
Pa_106**	495.66	270	1553	27	
Pa_8**	491.66	365	2593	27	
Pa_102**	492.66	525	4934	46	
Pa_105**	508.66	920	5749	43	
Bab 1***	486.65	440	2477	37	
Bab 2***	486.66	582	4526	30	
Bab 3***	488.67	738	6021	33	outlier
Bab 4***	44359	794	5884	22	
Bab 5***	44356	837	5887	26	
Bab 6***	5066.1	870	7577	52	outlier
Bab 7***	5067.1	1025	5025	33	outlier
Bab 8***	5064.1	1470	6500	32	
Bab 9***	5068.1	1546	6233	33	outlier
Sir_116****	1216.66	116	1558	35	
Sir_146****	5014.66	146	2201	32	
Sir_238****	1543.66	238	3139	32	
Sir_423****	1073.66	423	4711	38	
Sir_599****	1074.66	599	6735	44	
Sir_761****	1077.66	761	7254	41	

https://doi.org/10.5194/egusphere-2026-1693
Preprint. Discussion started: 16 April 2026
© Author(s) 2026. CC BY 4.0 License.

Table 1. Radiocarbon dates from LDF. The ages marked with stars were previously published (*** Hanganu et al., 2023; **** Preoteasa et al., 2021; ** Ţuţuianu et al., 2021; and * 2018). Comments indicate whether the 14C age was treated as outlier.

A total of 64 calibrated ^{14}C ages were considered, including 24 previously published dates (Hanganu et al., 2023; Preoteasa et al., 2021; Ţuţuianu et al., 2021, 2018) and 40 newly acquired measurements. All radiocarbon ages were calibrated in years before present (BP) using the IntCal20 calibration curve (Reimer et al., 2020). Fourteen dates were identified as outliers based on stratigraphic inconsistencies or large analytical uncertainties and were excluded from the final age model construction.

To account for non-linear sedimentation and stratigraphic constraints typical of dynamic floodplain environments, a Bayesian age–depth modeling approach was employed using the Bacon software package (Blaauw & Christen, 2011) in R. This method is particularly suited to sedimentary sequences with variable accumulation rates and allows the enforcement of stratigraphic ordering while incorporating dating uncertainties.

Based on the resulting age-depth models, 1-kyr isochrones were constructed for each sediment core. Isochrones were generated assuming that the top of each core corresponds to the time of sampling, enabling temporal alignment of stratigraphic and sedimentologic records across the study area.

These isochrones provide the basis for a temporally resolved analysis of sedimentological parameters, including grain-size distribution, sedimentation rates, and TOC concentrations, allowing their temporal evolution and relationships with geomorphological controls and floodplain carbon storage dynamics to be examined consistently across all cores.

4 Results

4.1 Stratigraphy and Facies Distribution

In this area, Holocene sediment thickness often exceeds 20–30 meters, surpassing the penetration capacity of our coring system. These deposits overlie a basal layer composed of coarse sands and gravels, likely deposited during the Late Glacial, when lower sea levels and steeper longitudinal gradients enhanced the sediment transport capacity of the Danube River. The basal coarse-grained sedimentary sequence has been documented in boreholes drilled since the 1950s by the National Research and Development Institute for Soil Improvement (ISPIF) across the Danube floodplain (Fig. 1). Above this basal unit, early Holocene sandy silts and silty sands accumulated, transitioning upward into predominantly silty middle- and late-Holocene floodplain deposits.

Building on this general stratigraphic framework, our sediment cores provide detailed insights into middle- and late-Holocene sedimentation. Eight cores were analyzed, with depths ranging from 8.0 to 18.75 m. Core locations, depths, and stratigraphic logs are shown in Fig. 1. Based on lithological characteristics and radiocarbon age constraints, three main stratigraphic units were distinguished:

https://doi.org/10.5194/egusphere-2026-1693
Preprint. Discussion started: 16 April 2026
© Author(s) 2026. CC BY 4.0 License.

The *basal unit* (>5000 cal BP) is dominated by silty sand and sand, typically massive or displaying subtle horizontal stratification. Notable exceptions occur in the JIJ, BP, and LC cores, where finer-grained (silty) deposits are more abundant. On average, sediments within this unit contain >60% silt, >25% sand, and approximately 10 % organic matter. Sedimentation rates are relatively high (~2.5 mm yr^{-1}), indicative of rapid floodplain aggradation during the first half of the middle-Holocene (Fig. 2).

The *intermediate unit* (5000–2000 cal BP) is dominated by structureless to finely laminated silts and clayey silts. Exceptions occur in two cores, where this interval consists entirely of peat (SMV) or is partially peat-bearing (PAR). This unit exhibits a clear fining-upward trend, with silt content approaching 75 % and clay content exceeding 10 % towards its upper sections. Mean organic matter content increases significantly to ~20 %, nearly double that of the underlying basal unit. Sedimentation rates decrease substantially to approximately 0.7 mm yr^{-1}, consistent with reduced sediment input and more uniform, fine-grained overbank deposition.

The *upper unit* (2000 cal BP–present) exhibits greater inter-core lithological variability, comprising alternations of silt, silty clay, and fine sand, as well as anthropogenically disturbed layers, including reworked topsoil horizons. On average, sediments in this unit contain around 75 % silt and nearly 15 % clay, whereas organic matter content declines to ~14 %. Sedimentation rates increase slightly to ~1.2 mm yr^{-1}, reflecting renewed floodplain instability and intermediate sediment input relative to the underlying units.

Based on grain-size characteristics (class frequency, mean grain-size, and sorting) and organic matter content, several sedimentary facies were identified within the studied cores: **(1) overbank deposits**, dominated by massive to faintly laminated silts with intercalated sand layers, typically indicative of periodic flood events and slow suspension settling; **(2) channel-fill deposits**, consisting of poorly sorted sandy-silty deposits displaying fining-upward trends, characteristic of channel abandonment phases; **(3) lacustrine deposits**, composed predominantly of finely laminated or massive moderately to well-sorted silts with subordinate clay, accumulated in standing-water conditions typical of floodplain lakes. In addition, intervals dominated by organic accumulation occur within various floodplain environments and are expressed as; **(4) organic-rich deposits** dominated by fine-grained, structureless or faintly laminated deposits with elevated organic matter content, indicative of slow accumulation in wetland conditions; and **(5) peat**, composed of fibrous organic matter with low mineral input, reflecting locally developed intervals of reduced clastic input and sustained vegetation accumulation (Fig. 1).

4.2 Carbon Content and Physical Properties of Sediments

In the statistical analysis of the total organic carbon (TOC) versus clay content and dry bulk density a positive linear correlation was observed between TOC and clay percentage (R^2=0.46; Fig. 4A). This relationship indicates that finer-grained sediments, particularly those enriched in clay, tend to retain higher amounts of organic carbon.

https://doi.org/10.5194/egusphere-2026-1693
Preprint. Discussion started: 16 April 2026
© Author(s) 2026. CC BY 4.0 License.

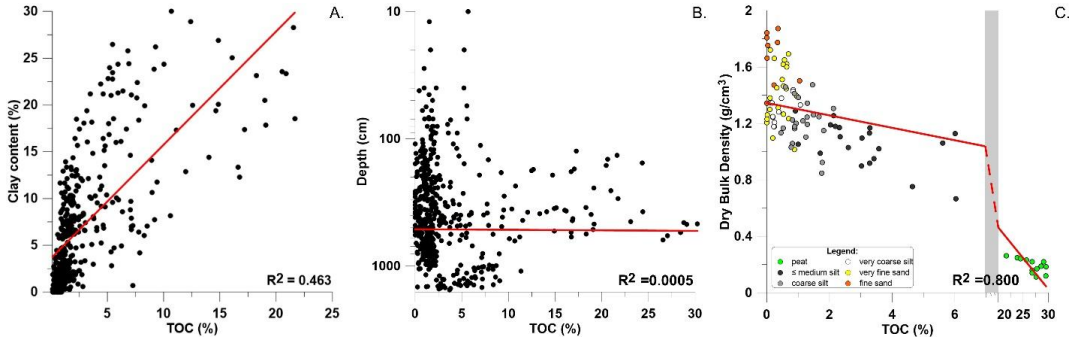

Figure 4. Relationships between TOC and selected physical properties of floodplain sediments. (A) TOC versus clay content, showing a positive relationship (R^2 = 0.463). (B) TOC versus depth, indicating no significant relationship (R^2 = 0.0005). (c) TOC versus dry bulk density, showing a strong inverse relationship (R^2 = 0.800). Point colours represent the mean grain-size class of each sample; grain-size analyses were not performed for peat or highly organic samples.

In contrast, no significant relationship was identified between TOC content and depth or age (R^2=0.0005; Fig. 4B). This finding is consistent with previous observations from floodplain and alluvial settings (Brevik & Homburg, 2004; Heger et al., 2021; Hoffmann et al., 2013), but contrasts with upland soil profiles, where TOC typically decreases with depth due to progressive decomposition and diminishing organic input (Jobbagy & Jackson, 2000). The absence of a depth-related TOC trend in the LDF suggests that carbon preservation is not primarily time-dependent. Instead, it reflects sediment properties and local depositional conditions at the time of accumulation. This pattern is characteristic of episodic floodplain sedimentation, where organic-rich layers are decoupled from cumulative burial depth.

Bulk density exhibits a strong inverse relationship with TOC in measured samples (R^2 = 0.80, Fig. 4C). Samples with bulk density values below 0.25 g cm^{-3} exhibit average TOC concentrations of up to 30 %, whereas samples exceeding 1.25 g cm^{-3} contain less than 0.6 % TOC. This trend reflects the combined effects of mineral dilution and the inherently low density of organic matter, emphasizing the role of sediment composition in controlling organic carbon concentrations.

With approximately 780 km^2 of the LDF under agricultural use, the uppermost metre of sediment cores from these sectors was examined in greater detail. Within the upper 50 cm, TOC values are systematically reduced, with the strongest decline observed at 20-30 cm depth, where concentrations are up to 2.5 times lower than those measured at 50–100 cm depth (Fig. 2).

4.3 Temporal and Facies-Controlled Carbon Accumulation

Over the past 7000 years, an estimated 58 Gt of total sediment has accumulated in the LDF, forming an average stratigraphic thickness of ~9.1 m. Of this total, approximately 1.7 Gt corresponds to organic carbon. According to the core-based chronological framework, more than half of the total sediment mass (60.8 %) was deposited prior to 5000 cal BP, while 22.2 % accumulated during the last 2000 years.

https://doi.org/10.5194/egusphere-2026-1693
Preprint. Discussion started: 16 April 2026
© Author(s) 2026. CC BY 4.0 License.

Carbon accumulation patterns closely mirror this temporal distribution of sediment deposition, but with pronounced shifts in organic carbon concentration and burial efficiency between phases. Prior to 5000 cal BP, TOC content averaged 4.2 %, while CAR were high (45.6 g C m^{-2} yr^{-1}), reflecting rapid floodplain sediment accumulation rates approaching ~3 mm yr^{-1}. Between 5000 and 2000 cal BP, TOC increased to 8.5 %, coinciding with a marked decline in sedimentation rate (0.6 mm yr^{-1}) and a reduced CAR of 16.1 g C m^{-2} yr^{-1}, consistent with enhanced floodplain stability. After 2000 cal BP, TOC decreased to 4.4 %, whereas CAR increased to 23.2 g C m^{-2} yr^{-1}, indicating a renewed increase in carbon burial driven by higher sedimentation rates (1.2 mm yr^{-1}) (Table 2).

Characteristic	Phase I:	Phase II:	Phase III:
Floodplain state	Geomorphically active floodplain system	Relative Geomorphic Stability	Quasi-stable floodplain morphology under anthropogenic regulation
Time interval (cal BP)	7000-5000	5000-2000	2000-present
Dominant driver	Post-glacial Sea-Level Rise	Base-Level Stabilization	Land use change/ direct anthropogenic intervention
Mean sedimentation rate (mm/yr)	2.9	0.6	1.2
Mean grain size (µm)	24.4	14.4	11.9
Mean TOC content (%)	4.2	8.4	4.4
Mean CAR (g C m^{-2} yr^{-1})	45.6	16.1	23.2

Table 2. Key sedimentological and carbon accumulation parameters for the three Holocene phases identified in the LDF, illustrating shifts in base-level dynamics, geomorphic activity, and anthropogenic influence.

Additional variation in TOC content and accumulation efficiency across sedimentary facies is illustrated in Fig. 5, highlighting differences between peat, organic-rich, lacustrine, overbank, and paleochannel (channel-fill) environments.

The ranges of TOC and CAR values are consistent with values reported from other large floodplain systems worldwide, including the Rhine, Nile, Amazon, and Sacramento–San Joaquin systems (Drexler, 2011; Eid et al., 2017; Hoffmann et al., 2009; Moreira et al., 2012).

5 Discussion

5.1. Sedimentological and Geomorphic Controls on Floodplain Carbon Accumulation

Carbon accumulation in the LDF is primarily controlled by sedimentological properties – particularly grain size and depositional energy – as well as by facies type, which together govern accumulation patterns.

https://doi.org/10.5194/egusphere-2026-1693
Preprint. Discussion started: 16 April 2026
© Author(s) 2026. CC BY 4.0 License.

The positive correlation between TOC concentrations and clay content observed in the LDF (Fig. 4A) highlights the key role of fine-grained sediments in organic matter preservation. Similar relationships have been documented in floodplain environments worldwide, including the Upper Rhine (Hoffmann et al., 2009), the Elbe floodplain (Heger et al., 2021) and North Carolina (Deiss et al., 2017), where TOC systematically increases with decreasing particle size. Fine-grained sediments provide extensive surface area for organo-mineral associations and promote low-oxygen microenvironments that limit microbial decomposition, thereby enhancing long-term preservation.

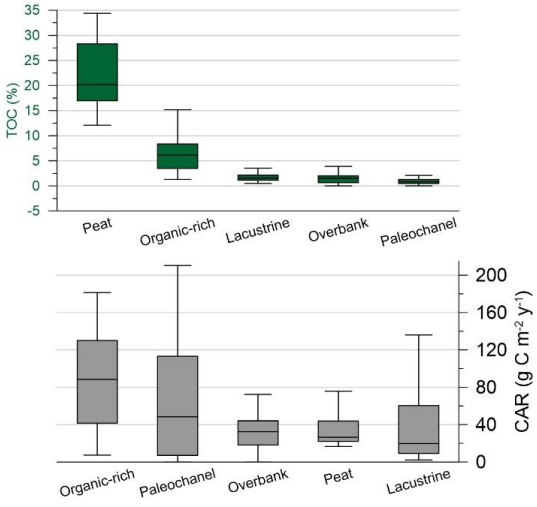

Figure 5. Distribution of total organic carbon (TOC) and carbon accumulation rates (CAR) across major depositional environments of the Lower Danube Floodplain.

This particle-size control is complemented by a strong inverse correlation between TOC and dry bulk density ($R^2 = 0.80$; Fig. 4C). Low-density, organic-rich facies (TOC > 12%, dry bulk density < 0.4 g/cm^3) typically form under anoxic to suboxic, low-energy settings. Comparable findings have been reported from North American floodplains (Wohl & Pfeiffer, 2018) and from the Nobi Plain in Japan (Hasada & Hori, 2016), underscoring the broad relevance of these sedimentary controls across diverse fluvial environments.

A particularly noteworthy finding is the absence of a statistically significant correlation between TOC and sediment depth ($R^2 = 0.0005$, Fig. 4B), in contrast to upland soils, where TOC typically declines with depth due to reduced organic inputs and sustained microbial degradation (Jobbagy & Jackson, 2000; Krüger et al., 2024; Lawrence et al., 2015). This finding is consistent with growing evidence that, in alluvial and wetland environments, carbon storage is decoupled from burial depth.

Recent studies demonstrate that shallow sampling depths can substantially underestimate floodplain soil organic carbon stocks. Bennett and Chambers (2023), for instance, show that limiting sampling to 50 or 100 cm underestimates soil organic carbon (SOC) stocks by 70 % and 48 %, respectively, with substantial carbon pools occurring at depths of 3–5 m. Similarly, D'Elia et al. (2017) report a 34 % increase in estimated SOC stocks in the Cosumnes River floodplain (California) when sampling depth is extended from 1 to 3 m. Together with our results, these observations indicate that vertical carbon distribution in floodplains is governed primarily by facies architecture and geomorphological setting rather than by progressive diagenetic loss with depth. Carbon-rich horizons reflect episodic depositional processes such as overbank flooding, temporary lacustrine phases, and peat development. These transitions between fluvial and wetland settings produce complex vertical carbon distributions that are decoupled from depth alone.

https://doi.org/10.5194/egusphere-2026-1693
Preprint. Discussion started: 16 April 2026
© Author(s) 2026. CC BY 4.0 License.

Another critical control is local hydrological connectivity, which strongly shapes spatial TOC distribution across the LDF by modulating oxygen exposure and redox conditions, sedimentation rates, and organic matter inputs. Areas subject to frequent or prolonged inundation – such as topographic depressions, abandoned channels, or infilled lake basins – consistently exhibit TOC values of 7–10 % higher than those of rarely flooded or well-drained environments. This pattern is consistent with observations from the Elbe floodplain (Heger et al., 2021) and the Austrian Danube floodplain (Tockner et al., 1999), where connectivity gradients exert a primary control on SOC stocks and the efficiency of organic matter retention.

These observations emphasize the central role of floodplain sedimentary processes and connectivity in shaping carbon accumulation and preservation within the LDF. Carbon storage is closely linked to sedimentary facies distribution, grain-size properties, depositional energy, and bulk density, all of which interact with local hydrological regimes to regulate organic carbon retention. Recognizing the importance of these process-based controls is essential for interpreting the pronounced spatial heterogeneity of TOC stocks in large river systems. At the same time, long-term trajectories of carbon accumulation in the LDF are also modulated by broader boundary conditions, particularly Holocene base-level changes and climate variability, which are addressed in the following section.

When viewed through a facies-based perspective (Fig. 5), the LDF clearly illustrates the functional decoupling between carbon concentration and long-term sequestration efficiency. Peat and organic-rich environments represent the organic end-members of the system, sustaining the highest TOC values under prolonged saturation and low-energy conditions. However, their limited clastic input constrains vertical accretion and thus moderates carbon accumulation rates (CAR). In contrast, paleochannel and overbank facies, despite comparatively lower TOC concentrations, benefit from sustained or episodic sediment supply, which enhances burial efficiency and elevates CAR. Lacustrine deposits occupy an intermediate textural position but tend to exhibit lower accumulation rates due to restricted sediment influx. These contrasts reinforce that floodplain carbon storage appears to be largely governed by the interaction between sediment delivery, accommodation space, and burial dynamics, rather than by organic enrichment alone.

5.2 Base-Level Change, Accommodation Space, and Long-Term Carbon Storage

The sedimentary record preserved in LDF cores spans the past ~7000 years and documents multiple phases of environmental change, during which carbon sequestration patterns closely follow variations in sea-level and sedimentation rate (Fig. 6A, F). Between 7000 and 5000 cal BP, corresponding to the final phase of postglacial eustatic sea-level rise, as indicated by relative sea-level trends derived from the ICE-7G_NA (VM7) glacio-hydro-isostatic model (Roy & Peltier, 2018), both sediment and carbon accumulation rates were remarkably high (Fig. 6A, C). More than 50 % of the total sediment mass and associated carbon stored in floodplain accumulated during this relatively short interval, despite low TOC concentrations (~4.2 %). This disproportionate accumulation reflects the creation of accommodation space in response to continued regional and global sea-level rise.

https://doi.org/10.5194/egusphere-2026-1693
Preprint. Discussion started: 16 April 2026
© Author(s) 2026. CC BY 4.0 License.

During this stage, carbon burial was primarily driven by carbon sequestration efficiency rather than biological productivity. The subsequent transition toward finer (Fig. 6D), more organic-rich deposits with lower accumulation rates is interpreted as reflecting base-level stabilization and the onset of near-equilibrium floodplain conditions – a sedimentary transition documented in many large fluvial and deltaic systems worldwide (Anthony et al., 2025; Drexler, 2011; Hasada & Hori, 2016; Rogers et al., 2019).

Following this early transgressive phase, the LDF entered a markedly different sedimentary regime between 5000 and 2000 cal BP. As the rate of sea-level rise slowed and stabilised, riverine influence became stronger at the river mouths, which entered a phase of progradation. Consequently, sedimentation rates in the upriver floodplain declined from ~1.6 mm/yr during the 6th millennium BP to just ~0.7 mm/yr in the 5th millennium BP.

At the same time, TOC concentrations nearly doubled, increasing from 3.5 % to an average of 6.2 %, clearly marking a regime shift from burial-driven to preservation-driven sequestration (Fig. 6B). Although sediment supply

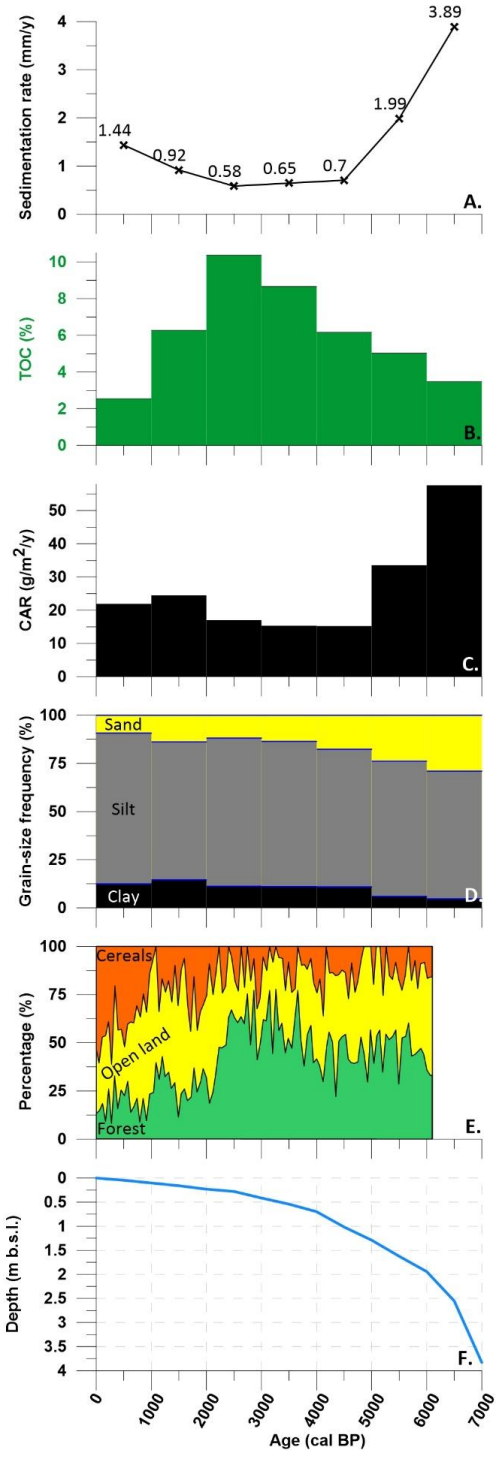

Figure 6. Multi-proxy reconstruction of carbon accumulation dynamics in the Lower Danube Floodplain over the past ~7000 years. (A) Sedimentation rates (mm yr⁻¹) derived from Bayesian age–depth models. (B) Mean total organic carbon content (TOC, %) and (C) carbon accumulation rates (CAR, g C m⁻² yr⁻¹) calculated for successive 1-kyr intervals. (D) Grain-size distribution expressed as cumulative frequencies of clay (black), silt (grey), and sand (yellow). (E) Percentage vegetation cover reconstructed using the REVEALS model from Lake Oltina (Feurdean et al., 2021), reflecting regional land-cover changes in the Lower Danube basin. (F) Relative Black Sea sea level trends derived from the ICE-7G glacio-hydro-isostatic model (Roy & Peltier, 2018).

https://doi.org/10.5194/egusphere-2026-1693
Preprint. Discussion started: 16 April 2026
© Author(s) 2026. CC BY 4.0 License.

likely remained constant, depositional environments with lower energy became dominant, promoting the accumulation of finer sediments and greater retention of organic matter under persistently shallow groundwater tables and saturated conditions (Blum et al., 2013).

Similar sedimentary transitions – from mineral-dominated to organic-rich facies – have been documented in other large river deltas and floodplains, including the Rhine–Meuse delta (Hijma et al., 2009), the Sacramento–San Joaquin system (Drexler, 2011), and the Yellow River delta (He et al., 2021). These examples point to a broader pattern in which floodplains experiencing stabilized or near-stabilized base levels and hydrological regimes preferentially accumulate higher TOC in fine-grained, low-energy depositional settings.

In the LDF, peat and organic-rich deposits from this interval likely formed in microtopographic depressions and low-lying floodplain areas subject to periodic overbank flooding, sustained by high groundwater tables and prolonged saturation. These settings resemble those described by Sutfin et al. (2016), where extended inundation and strong hydrological connectivity promote long-term carbon retention. Notably, CAR declined from ~45.6 to ~16.1 g C m^{-2} yr^{-1} (Fig. 6C), despite a marked increase in TOC concentrations (Fig. 6B). This decoupling between TOC concentration and burial efficiency highlights a critical dynamic: lower sedimentation rates constrain the absolute volume of carbon sequestered annually, even in organic-rich settings.

The decline of CAR to ~16.1 g C m^{-2} yr^{-1} during this interval likely represents the baseline sequestration capacity of the LDF under stable, low-energy hydrogeomorphic conditions prior to major anthropogenic disturbance. Comparable Holocene CAR ranges reported for the Rhine catchment (3.4–25.4 g C m^{-2} yr^{-1}; Hoffmann et al., 2009) support the interpretation that values around ~15–25 g C m^{-2} yr^{-1} are typical for large temperate European floodplains operating near geomorphic equilibrium.

After 2000 cal BP, the LDF stratigraphic record documents a shift toward more heterogeneous sediment textures, accompanied by a slight decrease in TOC (~4.4 %) and a renewed increase in CAR (~23.2 g C m^{-2} yr^{-1}). Although this interval spans several alternating warm and cold phases, the relative geomorphic stability of the floodplain suggests that climatic variability alone did not dominate carbon accumulation trajectories. Instead, intensifying human activity across the Danube basin increased erosion and sediment delivery, amplifying clastic input and driving the observed rise in CAR despite declining TOC levels.

Base-level change linked to Black sea-level evolution (Fig. 6F) emerges as a dominant external control shaping long-term carbon accumulation in the LDF, outweighing the influence of millennial-scale climate variability. The stratigraphic record offers a compelling case study of how base-level changes over the past 7000 years have governed both the volume and efficiency of carbon burial. Understanding this interplay between accommodation dynamics and preservation processes is essential for reconstructing past carbon budgets and anticipating future changes in floodplain systems. As contemporary rivers face intensifying hydrological alterations driven by global warming, river regulation, and land-use transformation, the LDF archive serves as a valuable analogue for assessing system sensitivity to external perturbations. Notably, the

https://doi.org/10.5194/egusphere-2026-1693
Preprint. Discussion started: 16 April 2026
© Author(s) 2026. CC BY 4.0 License.

attainment of the highest cumulative carbon burial during a phase of rapid sea-level rise suggests that, under favorable conditions of sediment supply and connectivity, rising base levels can enhance carbon sequestration in floodplain environments. However, as shown in the following section, human intervention has significantly altered catchment dynamics and disrupted hydrological connectivity, ultimately undermining the natural capacity of the LDF to function as a long-term carbon sink.

5.3 Anthropogenic Impacts and Management Perspectives

The long-term carbon accumulation history of the LDF reflects not only geomorphological and base-level controls, but also an increasingly influential anthropogenic footprint. This influence can be viewed as a historical paradox unfolding in two distinct acts: a first phase of unintended sequestration enhancement, followed by a second, modern phase characterized by the systematic disruption of carbon sinks. While carbon dynamics in floodplains have traditionally been examined through stratigraphic and biogeochemical lenses, it is now clear that anthropogenic modifications – both direct (e.g., embankment, channelization, drainage) and indirect (e.g., land-use change across the catchment) – exert a profound and often overriding influence on a floodplain's capacity to function as a long-term carbon reservoir.

5.3.1 Anthropogenic Influence and Enhanced Carbon Burial (c. 2000 cal BP – 20th Century)

Sedimentological evidence from LDF cores reveals a distinct shift beginning around 2000 cal BP, when both sedimentation rates and CAR rose again after a prolonged period of reduced accumulation. This reversal coincides with widespread land-use intensification throughout the Danube basin (Fig. 6E), as inferred from paleoecological and historical records (Kaplan et al., 2009; Feurdean et al., 2021; Hanganu et al., 2025). Accelerated deforestation, agricultural expansion, and grazing destabilized catchment slopes, triggering increased erosion and the delivery of vast quantities of "legacy sediment" into the fluvial system. The influx of mineral material promoted the burial of both in-situ organic matter and eroded topsoil carbon within the still-connected floodplain—a pattern similarly reported in other large European basins such as the Rhine (Hoffmann et al., 2009), Elbe (Heger et al., 2021), and the Austrian Danube (Cierjacks et al., 2010) as well as in tidal freshwater wetlands of the southeastern United States, where late Holocene land-use change enhanced sedimentation and carbon burial (Jones et al., 2017). During this long pre-industrial period, catchment degradation generated an increased sediment supply that enhanced carbon burial in the LDF.

5.3.2 The Era of Disconnection and Functional Decline (20th Century–Present)

The second, more recent, stage of anthropogenic transformation has had the opposite effect. Since the mid-20th century, large-scale hydraulic engineering – particularly the construction of dams such as Iron Gates I and II – has dramatically reduced sediment supply to the lower Danube, undermining the conditions that had previously favoured efficient carbon burial. At the same time, in the study area, extensive embankments and flood-control infrastructure have disconnected more than 85% of the historical floodplain from overbank flow, fundamentally altering the hydrological regime (Constantinescu et al., 2015). This "great disconnection" interrupted overbank sedimentation and disrupted the recurrent inundation cycles required for effective organic matter burial.

https://doi.org/10.5194/egusphere-2026-1693
Preprint. Discussion started: 16 April 2026
© Author(s) 2026. CC BY 4.0 License.

The drainage of formerly saturated floodplain surfaces has exposed long-buried, organic-rich horizons to oxygen, accelerating microbial decomposition and transforming formerly stable carbon sinks into carbon sources. This shift is reflected by TOC reductions of up to 2.5-fold within the upper 50 cm of agriculturally used floodplain sediments (Fig. 2, insert), where previously waterlogged layers are now regularly aerated and mechanically disturbed.

This marked functional degradation of the LDF stands in stark contrast to the resilience shown throughout the previous seven millennia. The paleo-record established here provides a critical long-term baseline against which the ecological and biogeochemical deterioration associated with 20th-century river regulation and land-use intensification can be evaluated.

5.3.3 Restoration as a Path Forward

Despite the profound anthropogenic alteration of the LDF, the stratigraphic and paleoenvironmental evidence presented here indicates that this trajectory is not irreversible. The sedimentary archive demonstrates that under natural or semi-natural hydrological connectivity – including past regimes of cyclical reconnection such as those described by Antipa (1910) – the system was capable of sustained organic-rich sediment accumulation and long-term carbon sequestration. These long-term observations are consistent with conceptual and empirical work showing that deltaic and floodplain systems can retain functionality when sediment delivery and hydrological connectivity are maintained or strategically enhanced, even under reduced sediment supply (Giosan et al., 2013).

Successful restoration cases illustrate the rate and magnitude at which floodplain systems can recover following reconnection. In the Cosumnes River floodplain (California), intentional levee breaches reinstated overbank flooding, triggering rapid sediment deposition and enhanced carbon burial (D'Elia et al., 2017). Similarly, in the Rhône delta (Camargue), the reconnection of wetlands to natural flooding regimes facilitated substantial recovery of soil organic carbon stocks and enhanced ecological resilience (Martínez-Eixarch et al., 2024). Together with conceptual models emphasizing the role of sediment partitioning and near-field controls on delta plain aggradation (Giosan et al., 2013), these examples underscore the responsiveness of floodplain carbon dynamics to relatively modest interventions aimed at restoring hydrological connectivity.

Overall, these findings highlight a fundamental lesson for the LDF: although extensive engineering and land-use change have substantially reduced its capacity to function as a carbon sink, targeted restoration – guided by geomorphic principles and focused on reconnecting floodplain surfaces to fluvial processes – offers a viable pathway for reversing this decline. Rehabilitated floodplains have the potential to regain multiple ecosystem functions, acting not only as long-term carbon sinks, but also as biodiversity hotspots, and buffers against hydrological extremes, offering a pathway for recovering ecological function at both regional and global scales. In this context, the LDF paleo-record provides a critical long-term benchmark for evaluating restoration potential and for designing process-based management strategies under future environmental change.

https://doi.org/10.5194/egusphere-2026-1693
Preprint. Discussion started: 16 April 2026
© Author(s) 2026. CC BY 4.0 License.

6 Conclusions

The analysed ~7000-year stratigraphic record from the Lower Danube Floodplain demonstrates that long-term carbon sink capacity is governed by the interplay of three dominant forcing regimes operating at different temporal scales.

(1) A burial-driven phase (7000–5000 cal BP), associated with post-glacial sea-level rise, high accommodation space, and rapid mineral sediment accumulation resulted in the most efficient carbon burial despite relatively low TOC concentrations.

(2) A preservation-driven phase (5000–2000 cal BP), characterised by reduced sedimentation rates, elevated TOC, and comparatively low CAR reflects stable hydrological conditions that favoured organic matter preservation but constrained overall carbon burial fluxes.

(3) A human-modified phase (last ~2000 years), during which widespread land-use change across the Danube basin enhanced sediment delivery and temporarily increased carbon burial, followed by a decline in sink functionality under modern river regulation and floodplain disconnection.

Facies-specific analyses reveal contrasting mechanisms of carbon storage across floodplain environments. Organic-rich backswamp deposits combine elevated TOC with relatively high CAR and therefore represent geomorphic carbon hotspots. Peat deposits exhibit the highest TOC but only moderate CAR, reflecting efficient carbon preservation under persistent saturation but limited burial rates. In contrast, paleochannel fills show the highest CAR despite low TOC, indicating burial-driven sequestration dominated by rapid sediment accumulation. Overbank and lacustrine facies display intermediate behaviour, with lower TOC and intermediate CAR, reflecting mixed controls of hydrology and depositional energy. These results demonstrate that carbon storage in large floodplains is primarily governed by the interaction between sedimentation rate, organic carbon concentration, and hydrological connectivity rather than burial depth.

The modern floodplain departs sharply from its Holocene behaviour. Hydrological disconnection, drainage and cultivation have aerated formerly waterlogged horizons, reduced TOC in the upper 50 cm by up to 2.5-fold and shifted parts of the system from a carbon sink toward a net carbon source. This recent deterioration highlights the sensitivity of floodplain carbon stores to river regulation and intensive land use.

Overall, the LDF record highlights both the resilience and fragility of large alluvial carbon sinks. While natural geomorphic–hydrological regimes can sustain long-term carbon accumulation, uncoordinated human modification rapidly erodes this function. The LDF therefore provides a valuable long-term reference for understanding floodplain carbon dynamics and suggests that effective restoration strategies should prioritize hydrological reconnection, sustained saturation, and geomorphically informed floodplain design in order to safeguard carbon storage and associated ecosystem services under ongoing environmental change.

https://doi.org/10.5194/egusphere-2026-1693
Preprint. Discussion started: 16 April 2026
© Author(s) 2026. CC BY 4.0 License.

Author contributions

Laurenţiu Ţuţuianu: Investigation, Data analysis, Writing – original draft, Writing – review & editing. Florin Zăinescu: Writing – review & editing. Alfred Vespremeanu-Stroe: Funding acquisition, Supervision, Writing – review & editing. Bogdan Ionel Stan: Data analysis, Writing – review & editing. Mihaela Dobre: Data analysis. Maria Luca-Ilie: Data analysis. Gabriela Sava: Data analysis. Cristian Mănăilescu: Data analysis. Luminiţa Preoteasa: Writing – review & editing.

Competing interests

The authors declare that they have no conflict of interest.

Acknowledgements

This research was supported by the PNRR-III-C9-2022-I8-CF253 (ChronoCaRP) project and by RO-NO-2019-0415 / Contract No. 30/2020 (ClimaLAND Project, EEA and Norway Grants). Radiocarbon measurements carried out at the 1MV Tandetron™ accelerator at the RoAMS Laboratory, „Horia Hulubei" National Institute for R&D in Physics and Nuclear Engineering (IFIN-HH) were supported by the Romanian Government Programme through the National Programme for Infrastructure of National Interest (IOSIN). "DELTA-HUB: River Delta Science, Education and Modeling Hub", funded by the European Union's Horizon Europe Research and Innovation Programme (Grant Agreement No. 101187110), is also acknowledged.
We thank our colleagues Daniel Ivanov and Alexandru Berbecariu for their support during fieldwork and sampling, Sabina Calisevici for her assistance with bulk density measurements, and Daniela Putici and Dan Olteanu for their help with sample preparation for total organic carbon (TOC) analyses.
ChatGPT-5 (OpenAI) and Grammarly were used for language editing only, helping with writing, including grammar correction and refining sentences and paragraphs. However, the original scientific ideas belong to the authors.

References:

Antipa, Gr., Regiunea inundabilă a Dunării, starea ei actuală şi mijloace de a o pune în valoare. Bucureşti, 1910.

Anthony, E., Syvitski, J., Cohen, K. M., Saito, Y., Zăinescu, F., Vespremeanu-Stroe, A., Nicholls, R. J., Marriner, N., Amorosi, A., Maselli, V., Minderhoud, P. S. J., Tamura, T., Day, J., Woodroffe, C. D., Preoteasa, L., Tatui, F., Sabatier, F., Morhange, C., Besset, M., Kemp, P., and Chen, Z.: A 7000-year record of human influence on Global River Deltas: Geomorphology, stratigraphy, the Anthropocene overprint and future, Earth-Science Rev., 271, https://doi.org/10.1016/j.earscirev.2025.105302, 2025.

Bennett, J. D. and Chambers, L.: Wetland soil carbon storage exceeds uplands in an urban natural area (Florida, USA), Soil Res., 61, 542–559, https://doi.org/10.1071/SR22235, 2023.

Blaauw, M. and Christeny, J. A.: Flexible paleoclimate age-depth models using an autoregressive gamma process, Bayesian Anal., 6, 457–474, https://doi.org/10.1214/11-BA618, 2011.

Blott, S. J. and Pye, K.: Gradistat: A grain size distribution and statictis package for the analysis of unconsolidated sediments, Earth Surf. Process. Landforms, 26, 1237–1248,

https://doi.org/10.5194/egusphere-2026-1693
Preprint. Discussion started: 16 April 2026
© Author(s) 2026. CC BY 4.0 License.

https://doi.org/10.1002/esp.261, 2001.

Blum, M., Martin, J., Milliken, K., and Garvin, M.: Paleovalley systems: Insights from Quaternary analogs and experiments, https://doi.org/10.1016/j.earscirev.2012.09.003, 2013.

Brevik, E. C. and Homburg, J. A.: A 5000 year record of carbon sequestration from a coastal lagoon and wetland complex, southern California, USA, Catena, 57, 221–232, https://doi.org/10.1016/j.catena.2003.12.001, 2004.

Busuioc, A., Caian, M., Cheval, S., Bojariu, R., Boroneant, C., Baciu, M. ,Dumitrescu, A., Climate Variability and Change in Romania. ProUniversitaria, ISBN: 978-973-129-549-7, 2010

Ciais, P., Sabine, C., Bala, G., Bopp, L., Brovkin, V., Canadell, J., Chhabra, A., DeFries, R., Galloway, J., Heimann, M., Jones, C., Quéré, C. Le, Myneni, R. B., Piao, S., and Thornton, P.: Carbon and Other Biogeochemical Cycles, Chang. IPCC Clim., 465–570, https://doi.org/10.1017/CBO9781107415324.015, 2013.

Cierjacks, A., Kleinschmit, B., Babinsky, M., Kleinschroth, F., Markert, A., Menzel, M., Ziechmann, U., Schiller, T., Graf, M., and Lang, F.: Carbon stocks of soil and vegetation on Danubian floodplains, J. Plant Nutr. Soil Sci., 173, 644–653, https://doi.org/10.1002/jpln.200900209, 2010.

Constantinescu, S., Achim, D., Rus, I., and Giosan, L.: Embanking the Lower Danube: From Natural to Engineered Floodplains and Back, Geomorphic Approaches to Integr. Floodplain Manag. Lowl. Fluv. Syst. North Am. and Eur., Spriger, 256–288, https://doi.org/10.1007/978-1-4939-2380-9, 2015.

D'Elia, A. H., Liles, G. C., Viers, J. H., and Smart, D. R.: Deep carbon storage potential of buried floodplain soils, Sci. Rep., 7, 1–7, https://doi.org/10.1038/s41598-017-06494-4, 2017.

Deiss, L., Franzluebbers, A. J., Amoozegar, A., Hesterberg, D., Polizzotto, M., and Cubbage, F. W.: Soil Carbon Fractions from an Alluvial Soil Texture Gradient in North Carolina, Soil Sci. Soc. Am. J., 81, 1096–1106, https://doi.org/10.2136/sssaj2016.09.0304, 2017.

Dong, Y., Li, H., He, H., and Wang, S.: Holocene peatland development, carbon accumulation and its response to climate forcing and local conditions in Laolike peatland, northeast China, Quat. Sci. Rev., 268, 107124, https://doi.org/10.1016/j.quascirev.2021.107124, 2021.

Drexler, J. Z.: Peat Formation Processes Through the Millennia in Tidal Marshes of the Sacramento-San Joaquin Delta, California, USA, Estuaries and Coasts, 34, 900–911, https://doi.org/10.1007/s12237-011-9393-7, 2011.

Eid, E. M., Keshta, A. E., Shaltout, K. H., Baldwin, A. H., and El-Din, A. A. S.: Carbon sequestration potential of the five Mediterranean lakes of Egypt, Fundam. Appl. Limnol., 190, 87–96, https://doi.org/10.1127/fal/2017/0993, 2017.

Esper, J., Torbenson, M., and Büntgen, U.: 2023 Summer Warmth Unparalleled Over the Past 2,000 Years, Nature, 631, https://doi.org/10.1038/s41586-024-07512-y, 2024.

Feurdean, A., Grindean, R., Florescu, G., Tanţău, I., Niedermeyer, E. M., Diaconu, A.-C., Hutchinson, S. M., Nielsen, A. B., Sava, T., Panait, A., Braun, M., and Hickler, T.: The transformation of the forest steppe in the lower Danube Plain of southeastern Europe: 6000 years

https://doi.org/10.5194/egusphere-2026-1693
Preprint. Discussion started: 16 April 2026
© Author(s) 2026. CC BY 4.0 License.

of vegetation and land use dynamics, Biogeosciences, 18, 1081–1103, https://doi.org/10.5194/bg-18-1081-2021, 2021

Fawzy, S., Osman, A. I., Doran, J., and Rooney, D. W.: Strategies for mitigation of climate change: a review, Environ. Chem. Lett., 18, 2069–2094, https://doi.org/10.1007/s10311-020-01059-w, 2020.

Folk, R. L. and Ward, W. C.: Brazos River Bar: A study in the significance of grain size parameters, J. Sediment. Petrol., 27, 3–26, 1957.

Fujimoto, K., Kawase, K., Ishizuka, S., Shichi, K., Ohira, A., and Adachi, H.: Sediment and carbon storages in the Yahagi River Delta during the Holocene, central Japan, Quat. Sci. Rev., 28, 1472–1480, https://doi.org/10.1016/j.quascirev.2009.01.012, 2009.

Giosan, L., Constantinescu, S., Filip, F., and Deng, B.: Maintenance of large deltas through channelization: Nature vs. humans in the Danube delta, Anthropocene, 1, 35–45, https://doi.org/10.1016/j.ancene.2013.09.001, 2013.

Goosse, H., Barriat, P. Y., Brovkin, V., Klein, F., Meissner, K. J., Menviel, L., and Mouchet, A.: Changes in atmospheric CO2 concentration over the past two millennia: contribution of climate variability, land-use and Southern Ocean dynamics, Clim. Dyn., 58, 2957–2979, https://doi.org/10.1007/s00382-021-06078-z, 2022.

Hanganu, D., Feurdean, A., Florescu, G. *et al.* Exploring human–landscape interactions in the Northern Balkans: Mostiștea Valley, from the Chalcolithic to Medieval Times, Veget Hist Archaeobot, https://doi.org/10.1007/s00334-025-01077-0, 2025.

Hanganu, D., Vespremeanu-Stroe, A., Feurdean, A., Brown, A. G., Țuțuianu, L., Rotaru, S., and Sava, G.: Mid-to late Holocene vegetation and environmental change at local and regional scales based on a multi-proxy analysis of the upper Danube Delta, Romania, Evol. Earth, 1, 100008, https://doi.org/10.1016/j.eve.2023.100008, 2023.

Hasada, K. and Hori, K.: Carbon storage in a Holocene deltaic sequence: An example from the Nobi Plain, central Japan, Quat. Int., 397, 194–207, https://doi.org/10.1016/j.quaint.2015.08.010, 2016.

He, L., Ye, S., and Laws, E. A.: Controlling Factors of Long-Term Carbon Sequestration in the Coastal Wetland Sediments of the Modern Yellow River Delta Area, China, Wetl. Carbon Environ. Manag. Geophys. Monogr., 191–212, https://doi.org/10.1002/9781119639305.ch10, 2021.

Heger, A., Becker, J. N., Vásconez Navas, L. K., and Eschenbach, A.: Factors controlling soil organic carbon stocks in hardwood floodplain forests of the lower middle Elbe River, Geoderma, 404, https://doi.org/10.1016/j.geoderma.2021.115389, 2021.

Heiri, O., Lotter, A. F., and Lemcke, G.: Loss on ignition as a method for estimating organic and carbonate content in sediments: reproducibility and comparability of results, J. Paleolimnol., 25, 101–110, https://doi.org/10.1023/A:1008119611481, 2001.

Hijma, M. P., Cohen, K. M., Hoffmann, G., Van der Spek, A. J. F., and Stouthamer, E.: From river valley to estuary : the evolution of the Rhine mouth in the early to middle Holocene (western Netherlands , Rhine-Meuse delta), Netherlands J. Geosci., 88, 13–53, http://doi.org/10.1017/S0016774600000986, 2009.

https://doi.org/10.5194/egusphere-2026-1693
Preprint. Discussion started: 16 April 2026
© Author(s) 2026. CC BY 4.0 License.

Hoffmann, T., Glatzel, S., and Dikau, R.: A carbon storage perspective on alluvial sediment storage in the Rhine catchment, Geomorphology, 108, 127–137, https://doi.org/10.1016/j.geomorph.2007.11.015, 2009.

Hoffmann, T., Schlummer, M., Notebaert, B., Verstraeten, G., and Korup, O.: Carbon burial in soil sediments from Holocene agricultural erosion, Central Europe, Global Biogeochem. Cycles, 27, 828–835, https://doi.org/10.1002/gbc.20071, 2013.

IPCC: Climate Change 2021: The Physical Science Basis. Contribution of Working Group I to the Sixth Assessment Report of the Intergovernmental Panel on Climate Change, Cambridge University Press, Cambridge, United Kingdom and New York, NY, USA, https://doi.org/10.1017/9781009157896, 2021.

Jobbagy, E. G. and Jackson, R. B.: The Vertical Distribution of Soil Organic Carbon and Its Relation to Climate and Vegetation, Ecol. Appl., 10, 423, https://doi.org/10.2307/2641104, 2000.

Jones, M. C., Bernhardt, C. E., Krauss, K. W., and Noe, G. B.: The Impact of Late Holocene Land Use Change, Climate Variability, and Sea Level Rise on Carbon Storage in Tidal Freshwater Wetlands on the Southeastern United States Coastal Plain, J. Geophys. Res., 3126–3141, https://doi.org/10.1002/2017JG004015, 2017.

Kaplan, J.O., Krumhardt, K.M., Zimmermann, N.,: The prehistoric and preindustrial deforestation of Europe, Quat. Sci. Rev., 28, 3016-3034, https://doi.org/10.1016/j.quascirev.2009.09.028, 2009.

Keogh, M. E., Törnqvist, T. E., Kolker, A. S., Erkens, G., and Bridgeman, J. G.: Organic matter accretion, shallow subsidence, and river delta sustainability, J. Geophys. Res. Earth Surf., https://doi.org/10.1029/2021jf006231, 2021.

Krüger, N., Finn, D. R., and Don, A.: Soil depth gradients of organic carbon-13 – A review on drivers and processes, Plant Soil, 495, 113–136, https://doi.org/10.1007/s11104-023-06328-5, 2024.

Lawrence, C. R., Harden, J. W., Xu, X., Schulz, M. S., and Trumbore, S. E.: Long-term controls on soil organic carbon with depth and time: A case study from the Cowlitz River Chronosequence, WA USA, Geoderma, 247–248, 73–87, https://doi.org/10.1016/j.geoderma.2015.02.005, 2015.

Longman, J., Veres, D., Haliuc, A., Finsinger, W., Ersek, V., Pascal, D., Sava, T., and Begy, R.: Carbon accumulation rates of Holocene peatlands in central-eastern Europe document the driving role of human impact over the past 4000 years, Clim. Past, 17, 2633–2652, https://doi.org/10.5194/cp-17-2633-2021, 2021.

Martínez-Eixarch, M., Masqué, P., Lafratta, A., Lavery, P., Hilaire, S., Jornet, L., Thomas, C., Boisnard, A., Pérez-Méndez, N., Alcaraz, C., Martínez-Espinosa, C., Ibáñez, C., and Grillas, P.: Assessing methane emissions and soil carbon stocks in the Camargue coastal wetlands: Management implications for climate change regulation, Sci. Total Environ., 950, https://doi.org/10.1016/j.scitotenv.2024.175224, 2024.

Mitra, S., Wassmann, R., and Vlek, P. L. G.: An appraisal of global wetland area and its organic carbon stock, Curr. Sci., 88, 25–35, 2005.

Mitsch, W. J. and Gosselink, J. G.: Wetlands (Fifth edition), 30–31 pp., https://doi.org/10.1108/rr-09-2015-0230, 2015.

https://doi.org/10.5194/egusphere-2026-1693
Preprint. Discussion started: 16 April 2026
© Author(s) 2026. CC BY 4.0 License.

Moreira, L. S., Moreira-Turcq, P., Turcq, B., Caquineau, S., and Cordeiro, R. C.: Paleohydrological changes in an Amazonian floodplain lake: Santa Ninha Lake, J. Paleolimnol., 48, 339–350, https://doi.org/10.1007/s10933-012-9601-x, 2012.

Nowacki, D., Langan, C. C. M., Kadereit, A., Pint, A., and Wunderlich, J.: "Lake Gorgana" - A paleolake in the Lower Danube Valley revealed using multi-proxy and regionalisation approaches, Quat. Int., 511, 107–123, https://doi.org/10.1016/j.quaint.2018.09.021, 2019.

Palomo, L. and Niell, F. X.: Primary production and nutrient budgets of Sarcocornia perennis ssp. alpini (Lag.) Castroviejo in the salt marsh of the Palmones River estuary (Southern Spain), Aquat. Bot., 91, 130–136, https://doi.org/10.1016/j.aquabot.2009.04.002, 2009.

Panait, A., Diaconu, A., Galka, M., Grindean, R., Hutchinson, S. M., Hickler, T., Lamentowicz, M., Mulch, A., Tanţău, I., Werner, C., and Feurdean, A.: Hydrological conditions and carbon accumulation rates reconstructed from a mountain raised bog in the Carpathians: A multi-proxy approach, Catena, 152, 57–68, https://doi.org/10.1016/j.catena.2016.12.023, 2017.

Preoteasa, L., Vespremeanu-Stroe, A., Dan, A., Ţuţuianu, L., Panaiotu, C., Stoica, M., Sava, T., Iancu, L. M., Stănică, A.-D., Zăinescu, F., Mirea, D. A., Olteanu, D. C., Pupim, F. N., and Ailincăi, S.: Late-Holocene landscape evolution and human presence in the northern Danube delta (Chilia distributary lobes), The Holocene, https://doi.org/10.1177/09596836211019121, 2021.

Pribyl, D. W.: A critical review of the conventional SOC to SOM conversion factor, Geoderma, 156, 75–83, https://doi.org/10.1016/j.geoderma.2010.02.003, 2010.

Radoane, M.: A history of the circum-pontic river channels marked by climate and sea level changes during the Late Quaternary (25-8 ka BP), Rev. Geomorfol., 23, 91-120, https://doi.org/10.21094/rg.2021.141, 2021.

Ramonet, M., Chatterjee, A., Ciais, P., Levin, I., Sha, M. K., Steinbacher, M., and Sweeney, C.: CO_2 in the Atmosphere: Growth and Trends Since 1850, 1–44 pp., https://doi.org/10.1093/acrefore/9780190228620.013.863, 2023.

Regnier, P., Friedlingstein, P., Ciais, P., Mackenzie, F. T., Gruber, N., Janssens, I. A., Laruelle, G. G., Lauerwald, R., Luyssaert, S., Andersson, A. J., Arndt, S., Arnosti, C., Borges, A. V., Dale, A. W., Gallego-Sala, A., Goddéris, Y., Goossens, N., Hartmann, J., Heinze, C., Ilyina, T., Joos, F., Larowe, D. E., Leifeld, J., Meysman, F. J. R., Munhoven, G., Raymond, P. A., Spahni, R., Suntharalingam, P., and Thullner, M.: Anthropogenic perturbation of the carbon fluxes from land to ocean, Nat. Geosci., 6, 597–607, https://doi.org/10.1038/ngeo1830, 2013.

Reimer, P. J., Austin, W. E. N., Bard, E., Bayliss, A., Blackwell, P. G., Bronk Ramsey, C., Butzin, M., Cheng, H., Edwards, R. L., Friedrich, M., Grootes, P. M., Guilderson, T. P., Hajdas, I., Heaton, T. J., Hogg, A. G., Hughen, K. A., Kromer, B., Manning, S. W., Muscheler, R., Palmer, J. G., Pearson, C., Van Der Plicht, J., Reimer, R. W., Richards, D. A., Scott, E. M., Southon, J. R., Turney, C. S. M., Wacker, L., Adolphi, F., Büntgen, U., Capano, M., Fahrni, S. M., Fogtmann-Schulz, A., Friedrich, R., Köhler, P., Kudsk, S., Miyake, F., Olsen, J., Reinig, F., Sakamoto, M., Sookdeo, A., and Talamo, S.: The IntCal20 Northern Hemisphere Radiocarbon Age Calibration Curve (0-55 cal kBP), Radiocarbon, 62, 725–757, https://doi.org/10.1017/RDC.2020.41, 2020.

Rogers, K., Kelleway, J. J., Saintilan, N., Megonigal, J. P., Adams, J. B., Holmquist, J. R., Lu, M., Schile-Beers, L., Zawadzki, A., Mazumder, D., and Woodroffe, C. D.: Wetland carbon storage

https://doi.org/10.5194/egusphere-2026-1693
Preprint. Discussion started: 16 April 2026
© Author(s) 2026. CC BY 4.0 License.

controlled by millennial-scale variation in relative sea-level rise, Nature, 567, 91–95, https://doi.org/10.1038/s41586-019-0951-7, 2019.

Romanescu, G.: Hydrological regime of the Prut River on the Romanian territory, Lucr. Semin. Geogr. Dimitrie Cantemir, 40, 5–22, https://doi.org/10.15551/lsgdc.v40i0.01, 2015.

Roy, K. and Peltier, W. R.: Relative sea level in the Western Mediterranean basin : A regional test of the ICE-7G _ NA (VM7) model and a constraint on late Holocene Antarctic deglaciation, Quat. Sci. Rev., 183, 76–87, https://doi.org/10.1016/j.quascirev.2017.12.021, 2018.

Sandu, I., Pescaru, V., Poiană, I., Geicu, A., Cândea, I., Țîătea, D., *Clima României*, Romanian Academy Publishing House, ISBN: 978-973-27-1674-8, 2008.

Sutfin, N. A., Wohl, E. E., and Dwire, K. A.: Banking carbon: A review of organic carbon storage and physical factors influencing retention in floodplains and riparian ecosystems, Earth Surf. Process. Landforms, 41, 38–60, https://doi.org/10.1002/esp.3857, 2016.

Tockner, K., Pennetzdorfer, D., Reiner, N., Schiemer, F., and Ward, J. V.: Hydrological connectivity, and the exchange of organic matter and nutrients in a dynamic river-floodplain system (Danube, Austria), Freshw. Biol., 41, 521–535, https://doi.org/10.1046/j.1365-2427.1999.00399.x, 1999.

Ţuţuianu, L., Vespremeanu-Stroe, A., Preoteasa, L., Rotaru, S., Dima, A., and Dimofte, D.: Wetlands and lakes formation and evolution on the Lower Danube Floodplain during Middle and Late Holocene, Quat. Int., https://doi.org/10.1016/j.quaint.2020.12.030, 2021.

Ţuţuianu, L., Stroe, A. V., Pendea, F., and Sava, T.: Mid and Late Holocene evolution of Brateș Lake region (Danube floodplain) based on the multiproxy analysis, Rev. Geomorfol., 20, 43–55, https://doi.org/10.21094/rg.2018.017, 2018.

Wang, Q., Li, Y., and Wang, Y.: Optimizing the weight loss-on-ignition methodology to quantify organic and carbonate carbon of sediments from diverse sources, Environ. Monit. Assess., 174, 241–257, https://doi.org/10.1007/s10661-010-1454-z, 2011.

Wohl, E. and Pfeiffer, A.: Organic carbon storage in floodplain soils of the U.S. prairies, River Res. Appl., 34, 406–416, https://doi.org/10.1002/rra.3269, 2018.